Probability of electrical breakdown: Evidence for a transition between the Townsend and streamer breakdown mechanisms

R. V. Hodges, R. N. Varney, and J. F. Riley
Lockheed Palo Alto Research Laboratory, Organization 93-50, Building 204, 3251 Hanover Street, Palo Alto, California 94304
(Received 12 September 1984)

Spark-breakdown delay times were measured for N_2, H_2, Ar, SF_6, and CCl_2F_2 in a uniform field gap provided with a small current ($\sim 10^{-15}$ A) of free electrons by uv illumination of the cathode. Laue plots of the delay times yielded straight lines with slope iP, where i is the photocurrent and P is the breakdown probability. The dependence of the breakdown probability on voltage for N_2, H_2, and Ar was in good agreement with predictions of the Townsend breakdown mechanism. In SF_6 and CCl_2F_2, a transition was observed with increasing pressure from a dependence that agreed with the Townsend theory to a more gradual rise with voltage, characteristic of a streamer mechanism. This transition was ascribed to a decrease in the secondary-ionization coefficient with increasing pressure in SF_6 and CCl_2F_2, which resulted in an average electron-avalanche size at the static breakdown voltage that approached the critical value for streamer formation. A unified breakdown-probability theory, for which the Townsend and streamer mechanisms are limiting cases, was developed to account for the data over the full pressure range. The implications of these results for measurement of the static breakdown voltage and the secondary-ionization coefficient are discussed.

I. INTRODUCTION

Under normal conditions a gas is a good electrical insulator. Electrical breakdown is the sudden transition of a gas to a conducting state. The ability of a gas to serve as either an insulator or a conductor has great technological significance. Controlled electrical breakdown is the basis of the operation of gas-filled switches. Interest in the physics of breakdown has increased because of the importance of high-power switches in fusion reactors, lasers, directed-energy weapons, and electromagnetic pulse generators.[1] Gases are used as insulation to prevent breakdown in high-voltage circuits and transmission lines. The probability of breakdown is an important consideration in the design of high-voltage systems.[2] A high probability of breakdown is required for the reliable performance of switches, whereas a very low probability of breakdown is necessary for insulation.

Electrical breakdown occurs when two conditions are satisfied.[3] First, the applied voltage must equal or exceed a minimum value (the static breakdown voltage V_s). Second, a free electron must be present in the gas. A free electron, accelerated by the electric field, produces more free electrons and positive ions in ionizing collisions with gas molecules. This process is described by the primary-ionization coefficient α, the average number of ionizing collisions experienced by one electron moving 1 cm along the direction of the electric field. An electron, departing from the cathode, creates an electron avalanche that grows exponentially to an average size $\bar{n}=\exp(\alpha d)$, where d is the electrode spacing. New avalanches are begun when positive ions, photons, or excited neutrals created in previous avalanches impinge on the cathode and eject electrons. This process is described by the secondary-ionization coefficient ω/α, the average number of secondary electrons released from the cathode per positive ion produced in the gas. Although the secondary-ionization coefficient is defined relative to the number of positive ions, its value includes the contributions of all secondary agents.

The development of current in a series of electron avalanches is the basis of the breakdown mechanism proposed in its initial form by Townsend.[4–7] The criterion for breakdown in the Townsend theory is that each electron avalanche produce on the average at least one secondary electron at the cathode, so that the discharge is self-sustaining. This criterion is expressed mathematically as

$$\mu=(\omega/\alpha)\bar{n}=1 \ . \tag{1}$$

Since α and ω are both functions of $V/(Nd)$, the Townsend criterion defines a breakdown voltage V_T, for a given gas number density N, and electrode spacing d.

The Townsend theory successfully accounted for the dependence of the breakdown voltage on gas density and electrode spacing. Other experimental evidence, however, was obtained which appeared to be inconsistent with the Townsend mechanism.[6–8] The time between application of voltage and electrical breakdown was measured. In spark gaps at atmospheric pressure with electrode spacing ~ 1 cm, very short delay times ($< 10^{-6}$ s) were obtained. Since positive ion transit times across the gap are $\sim 10^{-5}$ s, this time was too short to have involved a series of successive avalanches produced by ions impinging on the cathode. (Secondary action by photons was not considered.) Photographs of spark discharges revealed the existence of narrow, luminous "streamers" originating at the anode or in midgap, rather than the broad development from the cathode, expected for a Townsend discharge.

The streamer theory was developed to account for these and other observations.[6–9] In the streamer theory, breakdown occurs when one avalanche attains a critical size n_c. At the critical size, space charge creates regions of high

field around the head of the avalanche where free electrons can multiply efficiently. It was proposed that radiation from the avalanche produces free electrons by photoionization in these regions, propagating the avalanche to form the observed streamers. The production of secondary electrons at the cathode is not involved. The streamer breakdown criterion is

$$\bar{n}=n_c, \text{ or } (1/n_c)\bar{n}=1 . \quad (2)$$

It is apparent from Eqs. (1) and (2) that the form of the breakdown criteria of the two theories is the same. They differ in the mechanism of current growth in the prebreakdown stage of spark development: secondary electrons from the cathode (ω/α) in the Townsend model and a space-charge (n_c) induced process in the gas in the streamer model. The streamer theory has generated controversy because of the difficulty in quantitatively describing the ionization process.[6,7,10,11] The ability of an avalanche to produce photons energetic enough to ionize in a pure gas has been questioned.[10] Other ionization processes, associative ionization of excited atoms[12] and runaway electrons,[6,13] have been advanced to account for streamer propagation.

The calculation of breakdown probability in the framework of either of these breakdown mechanisms requires that the statistical nature of current development be considered. Although for many purposes collisional ionization in the gas and release of secondary electrons from the cathode may be represented by the average values α and ω/α, they are in reality stochastic processes. Current growth in an electrical discharge is subject to statistical fluctuations. A current flowing in the gas does not invariably lead to electrical breakdown even though the applied voltage exceeds V_s. Theoretical expressions for breakdown probability have been formulated for both the Townsend[14,15] and streamer[16,17] models.

Breakdown probability can be studied experimentally by measurements of the spark delay time. The time between application of voltage to a spark gap and collapse of the gap resistance is the sum of the statistical and formative delay times. The statistical delay time is the time between application of the voltage and the appearance of a free electron that initiates breakdown. The formative delay time is the time required for the current to build into a detectable discharge. Statistical delay times follow the distribution first applied by von Laue,[18]

$$N_t/N_0=\exp(-iPt) , \quad (3)$$

where N_t/N_0 is the fraction of delay times greater than t, i is the rate of appearance of free electrons, and P is the probability that an electron initiates breakdown. The average statistical delay time τ equals $1/iP$.

Many workers have reported measurements of statistical delay times in discharge gaps, but few have been done under conditions in which i was controlled so that P could be evaluated. If i is maintained constant, as by photoemission from the cathode, changes in the average delay time as a function of other parameters can be attributed to changes in P. We report here measurements of spark delay times as a function of voltage, pressure, and free electron current in N_2, H_2, Ar, SF_6, and CCl_2F_2. The results for N_2, H_2, and Ar were well described by the Townsend theory. The data for SF_6 and CCl_2F_2 fit the Townsend model at low pressure, the streamer model at higher pressure, and neither model at intermediate pressures. Good agreement was obtained over the entire pressure range with a new equation that combined elements of both the Townsend and streamer theories. The Townsend and streamer breakdown probabilities are limiting cases of this theory for ω/α large or zero. The results provide evidence for a transition between the two mechanisms and suggest the following regimes of validity: Townsend model for $\bar{n} \ll n_c$, and streamer model for $\bar{n} \geq n_c$. In the transition region both cathode secondary processes and space-charge field distortion are required to account for the data.

II. APPARATUS

The discharge gap and associated electronics are diagrammed in Fig. 1. The gap was contained in an aluminum chamber evacuated to a base pressure of 0.3 Pa (2 mTorr) by a mechanical pump. The cathode was a 1.25-cm-diam steel or molybdenum cylinder. The cathode surface was polished on a mechanical polishing wheel with 1-μm diamond paste, then cleaned with xylene and ethanol. The anode was a hollow steel cylinder with a 20-μm mesh (cut from a particle sieve) spot-welded to the end. This mesh size was sufficiently small to assure a uniform field over the electrode spacing of 0.5 mm. The accuracy of the spacing was estimated to be $\pm 10\%$.

Light from a Hg-Xe arc lamp passed through two apertures, a CaF window and the anode mesh, and struck the cathode surface, releasing photoelectrons. With the chamber evacuated and 20 V applied across the gap, pho-

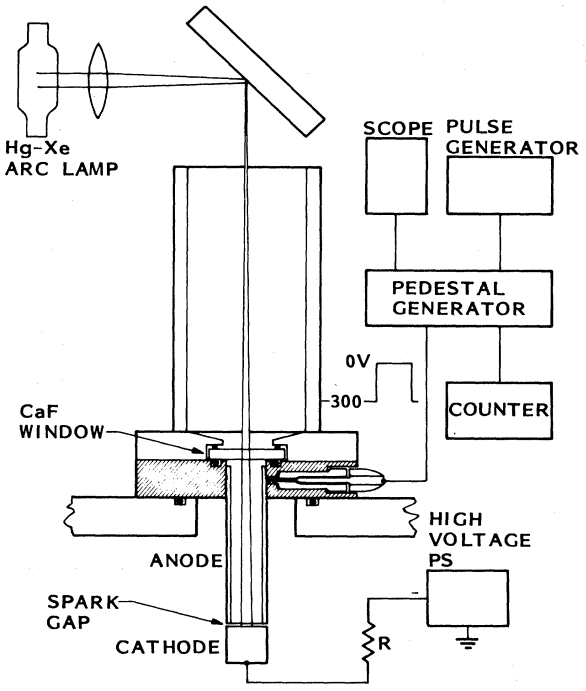

FIG. 1. Apparatus for measuring spark delay times.

tocurrents in the range 10^{-16}—10^{-14} A were measured with a Cary vibrating-reed electrometer. The photoelectron current was varied by placing wire screens in the light path. The attenuation factors of the screens were determined from measurements of the current with and without the screens in place.

The cathode was connected to an adjustable power supply through a quenching resistor (0.5—3.0 MΩ). The voltage on the anode was controlled by a custom-built voltage pedestal generator. A schematic of the operation of the pedestal generator and measurement of the spark delay time is shown in Fig. 2. A voltage of −300 V was applied to the anode so that the gap voltage was less than V_s. When the pedestal was activated manually with a button or automatically after a preset cycle time, the anode voltage was switched to ground. At the same time a logic gate opened, sending a 100-kHz square wave from a pulse generator to a counter. The pedestal remained on for a maximum of 300 ms. If breakdown occurred in less than 300 ms, the voltage pedestal was switched off and the gate to the counter was closed. The spark delay time was the ratio of the number of counts and the pulse generator frequency.

The following procedure was used to acquire the data. Gas was admitted to the discharge chamber to the desired pressure (read on a Wallace-Tiernan gauge). Research grade gases were used without further purification. The pedestal generator was set to trigger automatically every 5 sec and the cathode was gradually made more negative until breakdowns began to occur. Several hundred breakdowns were used to "condition" the cathode. Electrode damage was minimal since the only charge passed during the discharge was that stored on the gap capacitance. After conditioning, the chamber was evacuated and refilled. Spark delay times were measured and recorded manually beginning at the lowest voltage at which breakdowns were observed. Fifteen to forty measurements were made at each voltage. The voltage was increased in steps up to 250 V overvoltage, then decreased back to the minimum. Finally, measurements were repeated at one of the higher overvoltages to check that the photocurrent had not changed significantly. Delay times were occasionally measured with the light blocked and found to be much greater (usually >300 ms) than those with illumination. This confirmed that sources of electrons other than the photocurrent could be neglected.

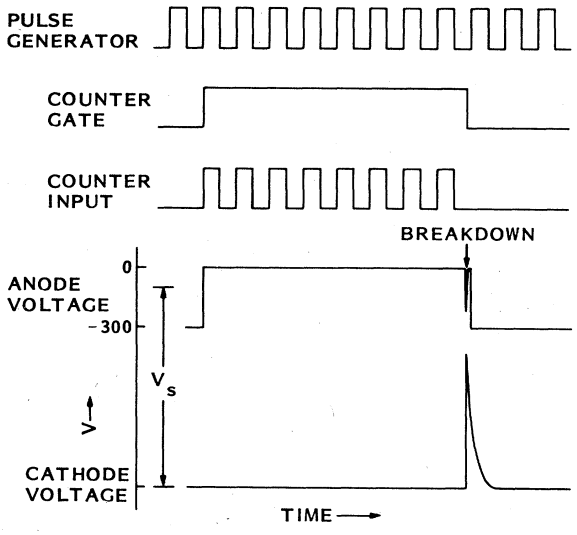

FIG. 2. Electrode voltages and timing circuit signals.

III. RESULTS

Plots of $\log(N_t/N_0)$ versus t yielded straight lines which were fit by the method of least squares. The slope, given by the Laue equation [Eq. (3)], is iP. The average delay time τ is the reciprocal of the slope, $1/(iP)$. Figure 3 shows Laue plots for three voltages in N_2 at 21.3 kPa (160 Torr). We assume that the photocurrent i is independent of voltage and that the differences in slope are due to different values of the breakdown probability P.

The dependence of the average delay time τ on the illumination intensity for N_2, SF_6, and CCl_2F_2 was measured at several different voltages. Results for SF_6 at two voltages are shown in Fig. 4. The average delay time was inversely proportional to the photocurrent, as predicted by the Laue equation [Eq. (3)] for statistical delay times. This verified that the formative delay time was negligible compared to the statistical delay time for these small photocurrents.

The dependence of the average delay times on voltage for several pressures of N_2, H_2, Ar, SF_6, and CCl_2F_2 is shown in Figs. 5—14. The right ordinate applies to the experimental points. Each point is the reciprocal of an average delay time and represents the slope of a plot like those in Fig. 3. For each of the curves in Figs. 5—14, as the applied voltage increases, the delay time approaches an asymptotic value which is determined by i (the rate of appearance of electrons) since the value of P is approaching one. The asymptotic value establishes the position of

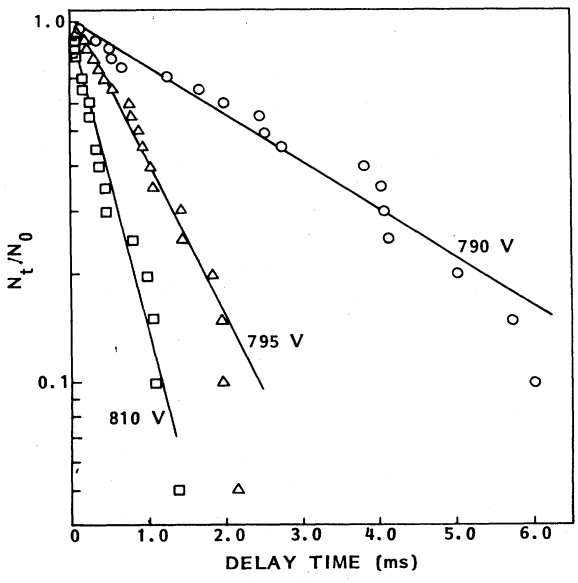

FIG. 3. Laue plots of spark delay times in N_2 at 21.3 kPa (160 Torr).

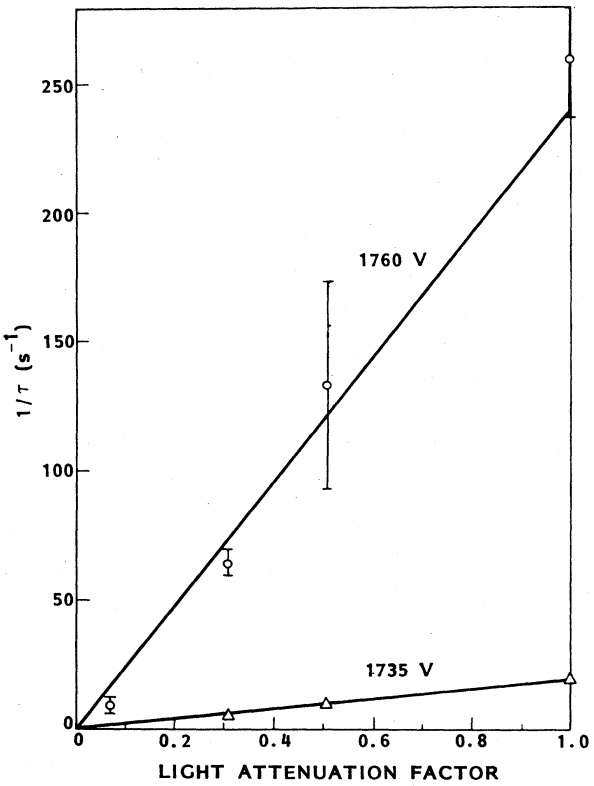

FIG. 4. Reciprocal of average spark delay time in 26.7 kPa (200 Torr) SF_6, electrode spacing 0.45 mm, as a function of cathode illumination intensity.

the scale of the left ordinate, which gives the breakdown probability. The major sources of experimental uncertainty are statistical variations and variations in the photocurrent. From the scatter of the experimental points about a smooth curve, we estimate the uncertainty in τ to be $\pm 30\%$. Longer conditioning periods usually resulted in reduced scatter.

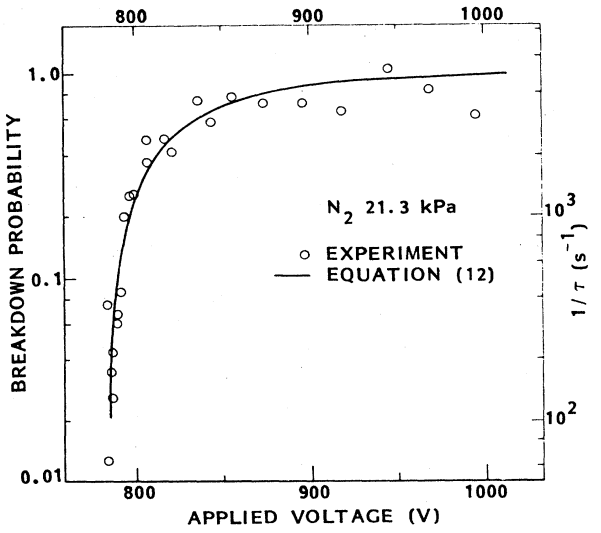

FIG. 5. Experimental average spark delay times and calculated initiation probabilities for N_2 at 21.3 kPa (160 Torr). Parameters: $d=0.45$ mm, $\omega/\alpha=1.2\times10^{-2}$.

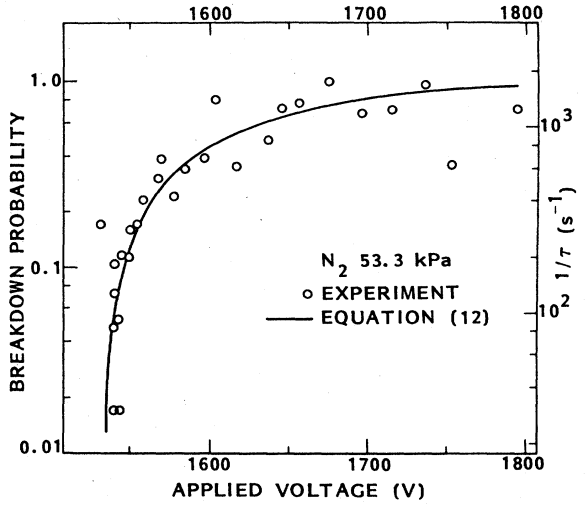

FIG. 6. Experimental average spark delay times and calculated initiation probabilities for N_2 at 53.3 kPa (400 Torr). Parameters: $d=0.45$ mm, $\omega/\alpha=2.9\times10^{-3}$.

The curves are calculated breakdown probabilities obtained from the equations discussed below. Literature values for α and η (the electron attachment coefficient) for N_2, H_2, Ar, SF_6, and CCl_2F_2 were taken from Refs. 19, 20, and 21, 19 and 22, and 23, respectively. The adjustable parameters in the calculations were ω/α and n_c. Although the nominal electrode spacing was 0.5 mm, significantly better fits were obtained for $d=0.45$ mm, which is within the experimental uncertainty.

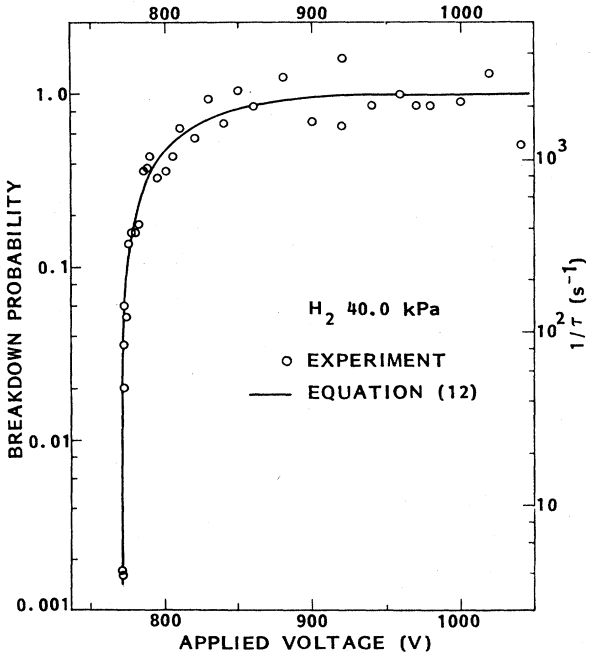

FIG. 7. Experimental average spark delay times and calculated initiation probabilities for H_2 at 40.0 kPa (300 Torr). Parameters: $d=0.45$ mm, $\omega/\alpha=1.2\times10^{-3}$.

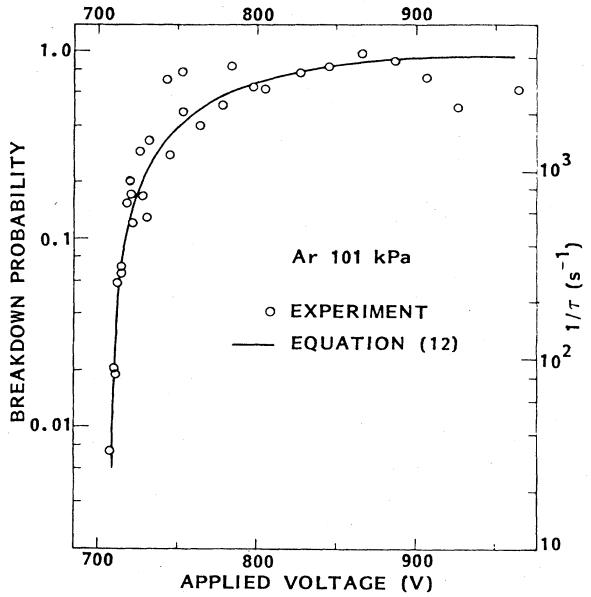

FIG. 8. Experimental average spark delay times and calculated initiation probabilities for Ar at 101 kPa (760 Torr). Parameters: $d=0.45$ mm, $\omega/\alpha=3.2\times10^{-2}$

IV. DISCUSSION

A. Theoretical breakdown probability

The statistics of avalanche growth. The stochastic nature of collisional ionization results in statistical variation in the growth of electron avalanches. The probability distribution $v(n)$ for the production of an avalanche of n electrons in a nonattaching gas is[14]

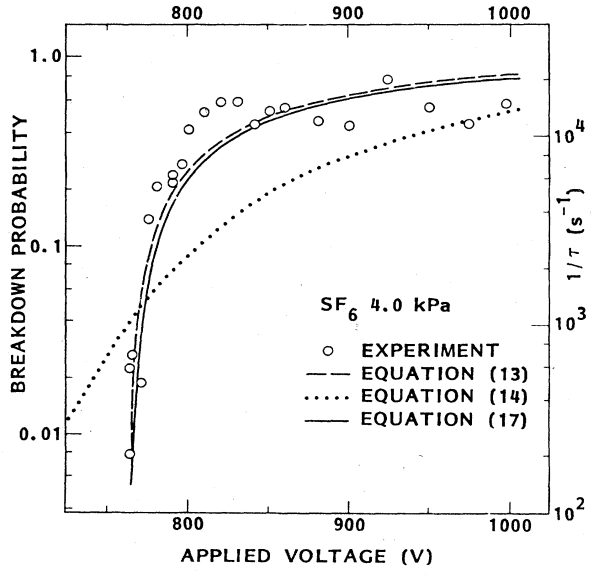

FIG. 9. Experimental average spark delay times and calculated initiation probabilities for SF_6 at 4.0 kPa (30 Torr). Parameters: $d=0.45$ mm, $\omega/\alpha=3.2\times10^{-5}$ [Eq. (13)], $\omega/\alpha=2.9\times10^{-5}$ [Eq. (17)], $n_c=1\times10^5$ [Eq. (14)], $n_c=5\times10^7$ [Eq. (17)].

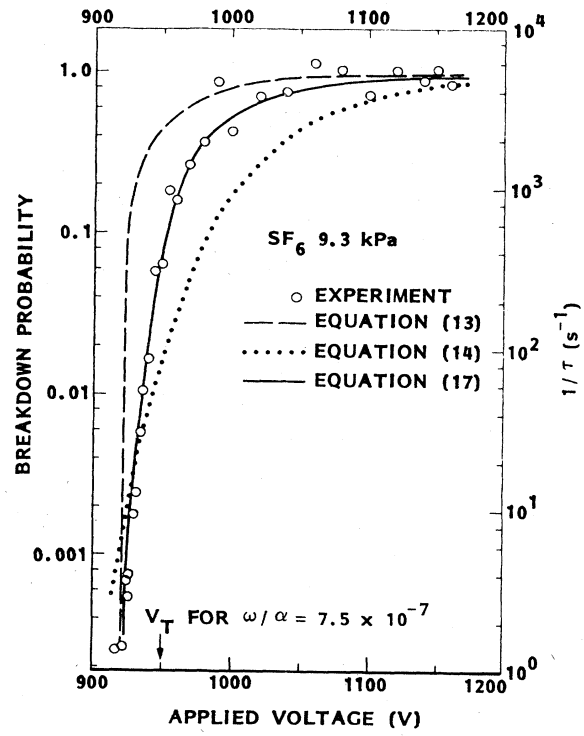

FIG. 10. Experimental average spark delay times and calculated initiation probabilities for SF_6 at 9.3 kPa (70 Torr). Parameters: $d=0.45$ mm, $\omega/\alpha=1.2\times10^{-6}$ [Eq. (13)], $\omega/\alpha=7.5\times10^{-7}$ [Eq. (17)], $n_c=5\times10^6$ [Eq. (14)], $n_c=5\times10^7$ [Eq. (17)].

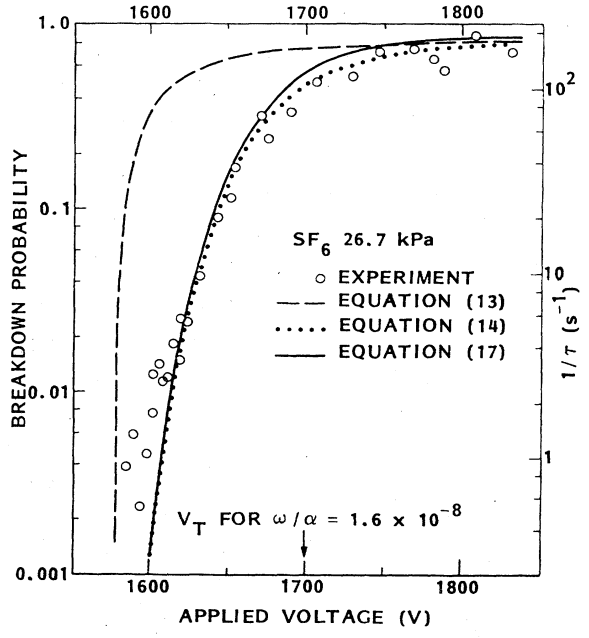

FIG. 11. Experimental average spark delay times and calculated initiation probabilities for SF_6 at 26.7 kPa (200 Torr). Parameters: $d=0.45$ mm, $\omega/\alpha=4.1\times10^{-7}$ [Eq. (13)], $\omega/\alpha=1.6\times10^{-8}$ [Eq. (17)], $n_c=3.3\times10^7$ [Eq. (14)], $n_c=5\times10^7$ [Eq. (17)].

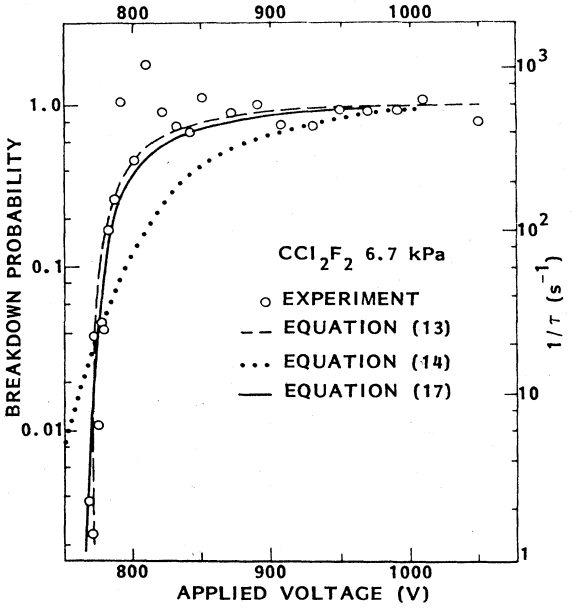

FIG. 12. Experimental average spark delay times and calculated initiation probabilities for CCl_2F_2 at 6.7 kPa (50 Torr). Parameters: $d=0.45$ mm, $\omega/\alpha=3.7\times10^{-6}$ [Eq. (13)], $\omega/\alpha=3.2\times10^{-6}$ [Eq. (17)], $n_c=1\times10^6$ [Eq. (14)], $n_c=5\times10^7$ [Eq. (17)].

$$v(n)=\frac{1}{\bar{n}}\left[1-\frac{1}{\bar{n}}\right]^{n-1}\sim\frac{1}{\bar{n}}\exp\left[\frac{n}{\bar{n}}\right], \tag{4}$$

where $\bar{n}=\exp(\alpha d)$. The number of positive ions in an avalanche is only one less than the number of electrons.

In electronegative gases negative ions are formed by attachment of electrons to neutral molecules. This process

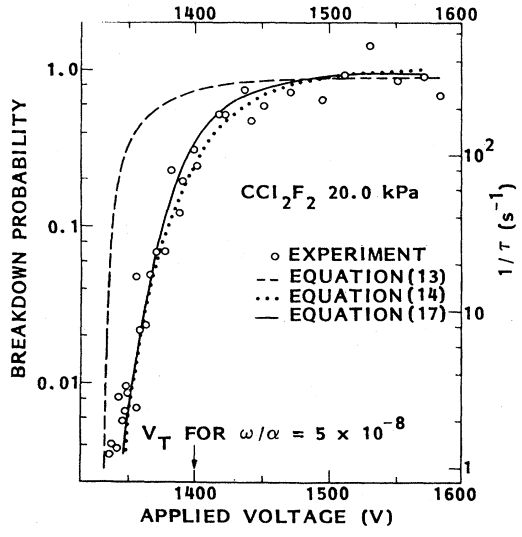

FIG. 13. Experimental average spark delay times and calculated initiation probabilities for CCl_2F_2 at 20.0 kPa (150 Torr). Parameters: $d=0.45$ mm, $\omega/\alpha=3.4\times10^{-7}$ [Eq. (13)], $\omega/\alpha=5\times10^{-8}$ [Eq. (17)], $n_c=2.8\times10^7$ [Eq. (14)], $n_c=5\times10^7$ [Eq. (17)].

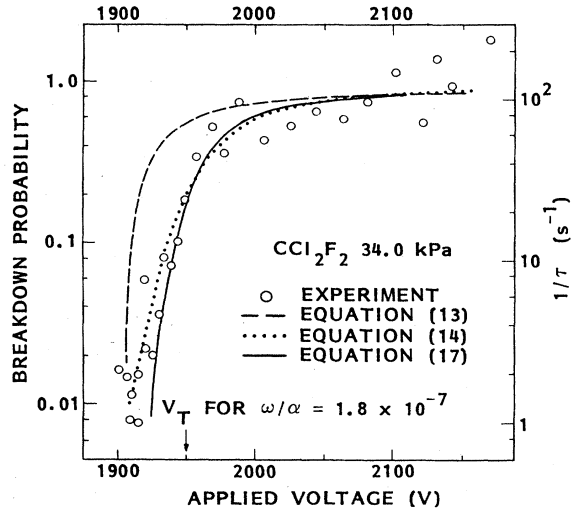

FIG. 14. Experimental average spark delay times and calculated initiation probabilities for CCl_2F_2 at 34.0 kPa (255 Torr). Parameters: $d=0.45$ mm, $\omega/\alpha=6.7\times10^{-7}$ [Eq. (13)], $\omega/\alpha=1.8\times10^{-7}$ [Eq. (17)], $n_c=1\times10^7$ [Eq. (14)], $n_c=5\times10^7$ [Eq. (17)].

is described by the attachment coefficient η, the number of attaching collisions per electron per centimeter travel in the direction of the electric field. The number of electrons and positive ions cannot be taken to be equal, but differ by the number of negative ions. In a fraction η/α of all avalanches, current development is aborted by attachment of all the electrons.[24] The average number of electrons and positive ions in *unaborted* avalanches is given by[24]

$$\bar{n}_e^*=\frac{\exp[(\alpha-\eta)d]}{1-\eta/\alpha} \tag{5}$$

and

$$\bar{n}_p^*=\frac{\exp[(\alpha-\eta)d]}{(1-\eta/\alpha)^2}\ . \tag{6}$$

The asterisks denote parameters in an electron-attaching gas. The Townsend breakdown criterion in attaching gases is

$$\mu^*=(\omega/\alpha)(1-\eta/\alpha)\bar{n}_p^*=1\ . \tag{7}$$

The probability distribution for electrons and positive ions is approximately[24]

$$v^*(n^*)=\begin{cases}\eta/\alpha & \text{for } n^*=0\\ (1-\eta/\alpha)\dfrac{1}{\bar{n}^*}\exp(-n^*/\bar{n}^*) & \text{for } n^*>0\ ,\end{cases} \tag{8}$$

with $n^*=n_e^*$ or n_p^*.

Townsend mechanism. Wijsman[14] and Legler[15] considered the stochastic nature of collisional ionization and secondary electron ejection from the cathode to calculate the breakdown probability. The probability $w(n_p,m)$ that an avalanche that produces n_p positive ions results in the release of m secondary electrons at the cathode is given by the binomial distribution

$$w(n_p,m)=\begin{bmatrix} n_p \\ m \end{bmatrix}(\omega/\alpha)^m(1-\omega/\alpha)^{n_p-m} . \quad (9)$$

Therefore, the probability $u(m)$ that the first avalanche produces m avalanches in the second generation is

$$u(m)=\sum_{n_p=0}^{\infty} w(n_p,m)v(n_p)=\frac{\mu^m}{(\mu+1)^{m+1}} . \quad (10)$$

In Wijsman's[14] and Legler's[15] derivation, electrical breakdown is defined as *the occurrence of an infinite succession of electron avalanches.* If $1-P$ is the probability that an avalanche series begun by one electron eventually terminates, the probability of termination of a series that has m avalanches in the second generation is $(1-P)^m$. Therefore,

$$1-P=\sum_{m=0}^{\infty} u(m)(1-P)^m . \quad (11)$$

The solution of this equation yields the probability of breakdown,

$$P=\begin{cases} 0 & \text{for } \mu \le 1 \\ 1-1/\mu & \text{for } \mu > 1 , \end{cases} \quad (12)$$

for nonattaching gases. This analysis was extended by Tagashira[25] to include electron attachment,

$$P^*=\begin{cases} 0 & \text{for } \mu^* \le 1 \\ (1-\eta/\alpha)(1-1/\mu^*) & \text{for } \mu^* > 1 . \end{cases} \quad (13)$$

Later Kondo and co-workers[26] considered the effect of detachment.

Electrical breakdown probabilities calculated from Eq. (12) or (13) are plotted with the experimental points in Figs. 5—14. There was good agreement between the experimental points and calculated curves for N_2, H_2, and Ar at all pressures and for SF_6 and CCl_2F_2 at lower pressures. As the pressure of CCl_2F_2 and SF_6 increased, a more gradual slope in the voltage dependence of the average spark delay time was observed, which was not predicted by Eq. (13).

These results are consistent with literature reports. Similar experiments showed agreement with Eq. (12) for N_2 (Refs. 27 and 28), Ne (Ref. 29), and H_2—rare-gas mixtures.[30] However, for SF_6 at 54 kPa (405 Torr) with electrode spacing 1.52 mm, Crowe[31] reported a more gradual slope resembling our higher-pressure results.

Streamer mechanism. Electrical breakdown in streamer theory is defined as *the occurrence of one avalanche that achieves the critical size.* The probability of electrical breakdown is the probability that a free electron produces an avalanche larger than the critical size n_c. The probability can be calculated from the integral of the avalanche-size distribution, which for electron-attaching gases is[17]

$$P^*=\int_{n_c}^{\infty} v^*(n^*)dn^*=(1-\eta/\alpha)\exp(-n_c/\bar{n}^*) . \quad (14)$$

Breakdown probabilities calculated from this equation for SF_6 and CCl_2F_2 with $\bar{n}^*=\bar{n}_p^*$ are plotted in Figs. 9—14. At the highest pressures agreement with experiment was good, but at the lower pressures Eq. (14) predicted a much more gradual slope than was measured and gave significant breakdown probabilities only with unreasonably small critical avalanche sizes $n_c \le 10^6$. This value is much below the critical size of 10^8 typical of streamer calculations.

A unified breakdown-probability theory. Neither the Townsend nor the streamer mechanisms alone can account for the behavior of the spark delay time in SF_6 and CCl_2F_2 over the full range of pressures investigated. The assumptions underlying either one of these mechanisms are not valid over the entire range. The streamer mechanism neglects secondary electrons produced at the cathode. The Townsend mechanism neglects field distortion by space charge. A more realistic description of the breakdown process is a buildup of space charge in a sequence of avalanches until the field distortion precipitates collapse of the gap voltage and establishment of a glow or arc discharge. We define electrical breakdown as *the occurrence of a sequence of avalanches in which the total number of positive ions produced achieves a critical value.* The drift velocity of ions is a factor of several hundred less than that of electrons. If the secondary electrons at the cathode are produced by photons [this is probably the case for SF_6 (Refs. 32 and 33)], the time between avalanche generations is approximately equal to the electron transit time. The positive ions from many generations of avalanches will accumulate in the gap.

Legler[34] has derived the expression for the probability distribution $V(n)$ of the total size of a *finite sequence* of avalanches as

$$V(n)=\frac{1}{\bar{n}}\frac{I_1(2\mu^{1/2}n/\bar{n})}{\mu^{1/2}n/\bar{n}}\exp[-(1+\mu)n/\bar{n}] , \quad (15)$$

where I_1 is the first-order Bessel function. The integral of the distribution over all n has one of two results depending on the sign chosen for a square root,[35]

$$\int_0^{\infty} V(n)dn=\begin{cases} 1 & \text{for } \mu \le 1 \\ 1/\mu & \text{for } \mu > 1 . \end{cases} \quad (16)$$

These results correlate with the probability for an infinite sequence [Eq. (12)]. For $\mu \le 1$, all avalanche sequences are finite, whereas for $\mu > 1$, the fraction $1-1/\mu$ is infinite.

The probability of electrical breakdown is the probability of an infinite avalanche sequence plus the probability of a finite sequence that achieves the critical size

$$P^*=\begin{cases} (1-\eta/\alpha)\int_{n_c}^{\infty} V(n_p^*)dn_p^* & \text{for } \mu^* \le 1 \\ (1-\eta/\alpha)\left[1-1/\mu^*+\int_{n_c}^{\infty} V(n_p^*)dn_p^*\right] & \text{for } \mu^* > 1 . \end{cases} \quad (17)$$

For electron-attaching gases the probability distribution $V(n)$ was multiplied by the factor $(1-\eta/\alpha)$, μ was replaced by μ^*, and $\bar{n}$ was taken to be the average number of positive ions $\bar{n}_p^*$. Note that this equation is not a simple sum of Eqs. (13) and (14), but includes finite *sequences* of avalanches with total size greater than n_c.

Unfortunately, an analytical solution of the indefinite

integral of $V(n)$ is not available. For $n_c\mu^{1/2}/\bar{n}$ large the integral can be approximated (see the Appendix). Calculated curves from Eq. (17) are plotted with the experimental data for SF_6 and CCl_2F_2 in Figs. 9–14. The agreement is good over the entire pressure range. The curves were fit by trial and error. The values given for the parameters are reasonable, but are not necessarily unique.

The distinction between finite and infinite avalanche sequences has mathematical, but not physical significance, since, of course, all real avalanche sequences are finite ones, which either die out or build up current to the point of voltage collapse. The mathematical distinction is useful to show the relationship between Eq. (17) and the Wijsman-Legler theory, which includes only infinite sequences. Figure 15 shows separately the contributions of finite and infinite sequences of avalanches to the total theoretical breakdown probability from Eq. (17) for SF_6 at 27.6 kPa (see Fig. 11). At voltages below V_T, $\mu^* < 1$ and only finite sequences contribute to the breakdown probability. Above V_T the probability of an infinite sequence is nonzero and the fraction of finite avalanches decreases.

The Townsend and streamer breakdown probabilities are limiting cases of the unified theory. For $\omega/\alpha=0$ (no cathode secondary effect), $\mu=0$ and $V(n)=v(n)$, so that Eq. (17) becomes the streamer probability, Eq. (14). For ω/α large, breakdown occurs by the Townsend mechanism at a voltage at which $\bar{n}$ is still much smaller than n_c. Many avalanches are required to accumulate the critical space charge, and finite avalanche series make a negligible contribution to the breakdown probability, i.e., $\int_{n_c}^{\infty} V(n)dn \sim 0$.

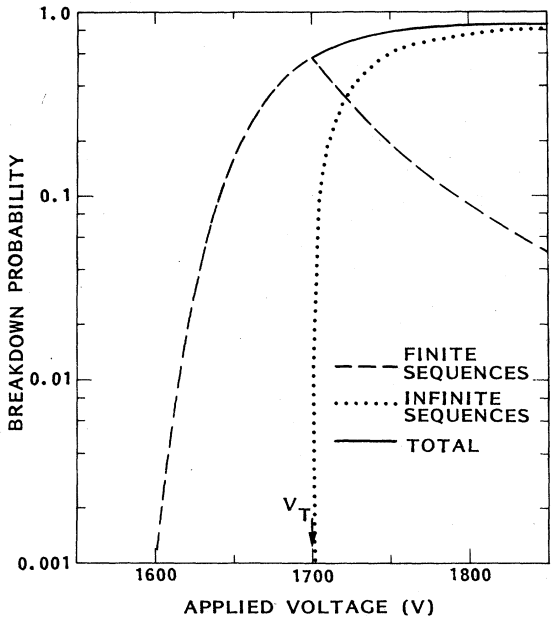

FIG. 15. Contributions of finite and infinite avalanche sequences to the calculated breakdown probability in SF_6 at 26.7 kPa (see Fig. 11).

B. Transition between the Townsend and streamer mechanisms

There has been much discussion in the literature regarding the conditions under which the Townsend and streamer mechanisms apply.[6,7] Townsend's work was carried out at low voltages that required the use of low gas densities and small electrode spacings. With the development of high-voltage techniques, the range of experimental data was extended to larger Nd. The difficulties in interpreting these results by the Townsend mechanism led to the proposal of the streamer theory. The first proponents[8] of the streamer theory suggested a transition between the two mechanisms in air at $Nd = 6.6\times10^{18}$ cm^{-2} (200 Torr cm), with the Townsend mechanism being valid below this value and the streamer mechanism applying at larger values. More recently measurements of formative delay times as a function of Nd and voltage have suggested a different boundary.[36] Discontinuities in delay time versus voltage curves were observed and attributed to a transition between the two mechanisms with overvoltage, rather than Nd, being the critical parameter. The Townsend mechanism was considered valid for low overvoltage ($<20\%$), the streamer mechanism at high overvoltage ($>20\%$).[6]

The present results represent another type of experiment that provides evidence for a transition between the two mechanisms. The breakdown probabilities in Figs. 9–11 and 12–14, respectively, show a transition at low overvoltages from a voltage dependence consistent with the Townsend model [Eq. (13)] to a dependence which fits the streamer equation [Eq. (14)]. The unified theory [Eq. (17)] describes the transition. The dominant character of Eq. (17) depends on the relative values of the average avalanche size $\bar{n}$ and the critical space charge n_c. For $\bar{n} \ll n_c$ many avalanche generations are required to accumulate sufficient space charge and the Townsend equation is an acceptable approximation. As $\bar{n}$ approaches n_c the probability that one avalanche is large enough to cause breakdown becomes significant and the effect of space charge must be included. This suggests the regimes of validity of the two models: Townsend theory for $\bar{n} \ll n_c$ and streamer theory for $\bar{n} \geq n_c$. This definition of the transition is equivalent to the assignment of the models to different ranges of overvoltage, since $\bar{n}$ is a strong function of voltage. The overvoltage at which the transition occurs depends on the relative values of ω/α and $1/n_c$. If ω/α is so small that the Townsend criterion is not satisfied until $\bar{n}$ approaches n_c, the influence of space charge will be important at 0% overvoltage.

Raether has discussed this transition in similar terms.[9] Methane and ether ordinarily have a very low ω/α, so that the streamer mechanism is valid at the static breakdown voltage. However, if a copper cathode is coated with CuI to increase ω/α, successions of Townsend avalanches can be observed in these gases.[37]

The application of this principle to SF_6 is illustrated in Fig. 16. Our experimental breakdown voltage measurements and those of Bhalla and Craggs[38] are used to construct a Paschen curve giving the value of E/N at breakdown as a function of Nd. Calculated curves are also

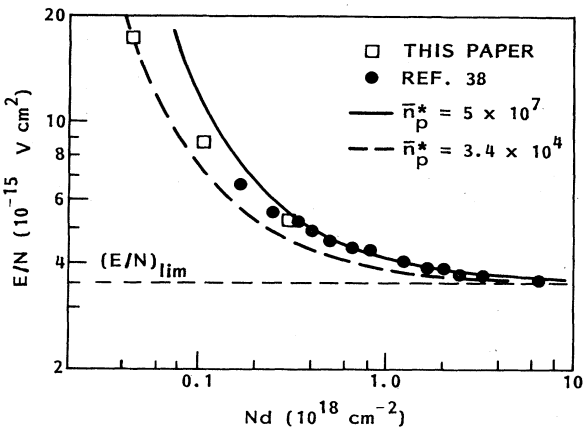

FIG. 16. E/N at the static breakdown voltage as a function of Nd for SF_6.

plotted that show the values of E/N and Nd that satisfy the condition $\bar{n}_p^* = \text{const}$. The solid curve represents $\bar{n}_p^* = n_c = 5\times10^7$, which is the value for the critical avalanche size that gave reasonable fits to the data in Figs. 9—11. The dashed curve, which passes through our experimental breakdown voltage at 4 kPa ($Nd = 4.5\times10^{16}$ cm^{-2}), is shown for comparison and represents $\bar{n}_p^* = 3.4\times10^4$. These curves are members of the family of curves defined by the equation $k\bar{n}_p^* = 1$, where k is a constant. Comparison with the breakdown criteria, Eq. (1) or (2), shows that these curves give the Paschen curves expected if ω/α or $1/n_c$ were constant. The experimental points for SF_6 do not lie on a single curve, but fall on curves of smaller k with increasing Nd. The value of ω/α obtained from fits of the probability curves in Figs. 9—11 decreases from 2.9×10^{-5} at 4 kPa (30 Torr) to 1.6×10^{-8} at 26.7 kPa (200 Torr). A similar trend occurs in CCl_2F_2. A decrease in ω/α with increasing pressure is characteristic of a photon secondary effect, which is reduced by increased collisional quenching of photon-emitting excited states and absorption of photons in the gas.[32,33,39] The decrease may also be due to increased electron attachment near the cathode surface.

The transition from Townsend to streamer behavior with increasing pressure in SF_6 and CCl_2F_2 is a consequence of the decrease in ω/α, which causes the Paschen curve to approach the line $\bar{n}_p^* = n_c$ (Fig. 16). In SF_6 at 4 kPa ($Nd = 4.5\times10^{16}$ cm^{-2}) with $\omega/\alpha = 2.9\times10^{-5}$, breakdown occurs by the Townsend mechanism at $\bar{n}_p^* \ll n_c$. The breakdown probability is well described by the Townsend model [Eq. (13)] and $V_s = V_T$ (Fig. 9). Transition to a streamer mechanism will occur at an overvoltage at which $\bar{n}_p^*$ approaches n_c. At 9.3 kPa ($Nd = 1.05\times10^{17}$ cm^{-2}), $\omega/\alpha = 7.5\times10^{-7}$ and satisfaction of the Townsend criterion requires an average avalanche size $\bar{n}_p^* \sim 10^6$. The probability that only a few avalanche generations produce space-charge field distortion is significant. Both secondary action at the cathode and space-charge field distortion are required to account for the dependence of the breakdown probability on voltage (Fig. 10). A significant breakdown probability exists below the voltage at which the Townsend criterion is satisfied, i.e., $V_s < V_T$. At 26.7 kPa ($Nd = 3.0\times10^{17}$ cm^{-2}) a value for the secondary-ionization coefficient, $\omega/\alpha = 1.6\times10^{-8}$, gives a reasonable fit to the data (Fig. 11). An average avalanche size approximately equal to n_c would be required to satisfy the Townsend criterion. Space charge dominates breakdown at the static breakdown voltage and the streamer breakdown probability fits the experimental data. Chalmers and co-workers[40] investigated spark development in SF_6 at $Nd = 10^{19}$ cm^{-2} by time-resolved photography and found evidence for space-charge field distortion in early stages of current growth at low overvoltage.

These considerations also apply to measurements of ω/α, obtained from the Townsend breakdown criterion [Eq. (1)] or from the curvature in plots of prebreakdown currents. Several authors[33,38,41,42] have reported values for SF_6 and CCl_2F_2 in the range 10^{-9}—10^{-7}. It is likely that space-charge field distortion affected these measurements. The Townsend criterion cannot be used if $V_s < V_T$. Varney and co-workers[43] have shown that upcurving in plots of prebreakdown current can be caused by distortion of the field by space charge.

C. Breakdown probability and the critical nature of the static breakdown voltage

The breakdown criteria [Eqs. (1) and (2)] are ordinarily interpreted to define a critical voltage V_s, below which breakdown will not occur. However, because of the stochastic nature of current growth, the breakdown probability is not a step function from 0 to 1 at this voltage, but increases over a range of voltages. The probability function P must be considered in the interpretation of measurements of V_s.

The outstanding characteristic of our experimental data is the markedly more gradual rise of $\log P$ versus voltage seen particularly in Figs. 11 and 14 for higher pressures in SF_6 and CCl_2F_2. We have attributed this difference to the onset of space-charge effects (streamer breakdown). It is notable that, according to the Townsend theory, there is a well-defined voltage threshold for breakdown, shown in Eq. (12), wherein the breakdown probability is zero for $\mu \le 1$. Above the threshold the probability rises extremely rapidly, so that the critical nature of the threshold is only mildly affected by statistical factors. There is no such clearly marked threshold shown in the streamer case, Eq. (14), for which the breakdown probability varies as $\exp(-n_c/\bar{n})$, which declines progressively more steeply as $\bar{n}$ decreases, but still never becomes precisely zero.

The relationship of the breakdown-probability equations to the measurement of the breakdown voltage is illustrated in the following calculation. A common procedure for measuring V_s is to apply a slowly rising voltage ramp to a spark gap which is irradiated to provide initiating electrons. The distribution function of the measured breakdown voltage is given by

$$F(V) = 1 - \exp\left[-\int_0^V \frac{i(V')P(V')}{dV'/dt}dV'\right], \tag{18}$$

where $F(V)$ is the fraction of measurements that exceed

V, i is the rate of appearance of free electrons, and P is the breakdown probability. In this equation the assumption is made that the free electrons act independently. This assumption will be valid for $i < 1/t_f$, where t_f is the formative delay time.

Distribution functions were calculated for N_2 at 53.3 kPa (400 Torr) and SF_6 at 26.7 kPa (200 Torr) at $d = 0.45$ mm for a ramp rate of 1 V/s and for $i = 1$ electron/s and $i = 6.24 \times 10^6$ electron/s (1 pA) (Fig. 17). For N_2 with 1 electron/s a spread of several volts is predicted, but with 1 pA of free electrons the distribution rises very steeply and is indistinguishable from a step function within experimental voltage resolution. Under the latter conditions the breakdown voltage measurement will yield a critical voltage nearly identical with V_T. Davies and Evans also found that the statistical uncertainties in the Townsend model are negligible in measurements of V_s, if a sufficient number of free electrons are present.[44]

A different situation occurs with SF_6 at 26.7 kPa in which space charge is significant. The streamer breakdown probability does not define a critical voltage below which the breakdown probability is zero. The more gradual rise of the probability curve results in measured breakdown voltages that depend strongly on experimental conditions.

V. CONCLUSIONS

The breakdown mechanism near the static breakdown voltage can be identified by the voltage dependence of the breakdown probability. The Townsend mechanism predicts a well-defined voltage threshold for breakdown above which the probability rises rapidly from zero to one. The probability of streamer breakdown does not have a precise threshold and increases less steeply with overvoltage. The breakdown probabilities measured in N_2, H_2, and Ar agreed with the Townsend probability equation. In SF_6 and CCl_2F_2 a transition was observed between Townsend and streamer behavior with increasing pressure. A unified probability theory, for which the Townsend and streamer mechanisms are limiting cases, accounted for the transition. The results of this paper do not depend on the *mechanism* of streamer propagation, but rather suggest the *conditions* under which space charge affects the prebreakdown state of current growth.

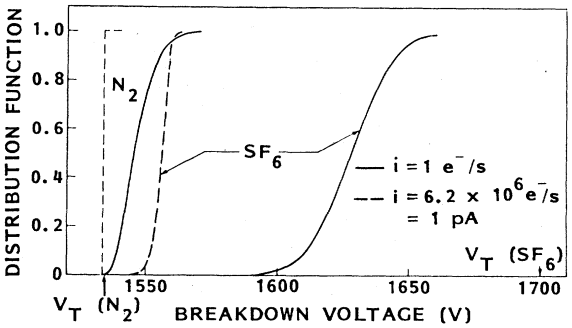

FIG. 17. Breakdown voltage distribution functions calculated from Eq. (18) for N_2 and SF_6 for a voltage ramp rate of 1 V/s.

(1) Breakdown occurs by the Townsend mechanism if the average avalanche size $\bar{n}$ is much smaller than the critical size for streamer formation n_c. As $\bar{n}$ approaches n_c the probability of rapid streamer breakdown becomes significant.

(2) The overvoltage at which the transition to streamer breakdown occurs depends on the relative values of n_c and the secondary-ionization coefficient ω/α. If $\omega/\alpha \leq 1/n_c$, breakdown at the static breakdown voltage V_s will occur by the rapid streamer process.

(3) When $\omega/\alpha < 10^{-7}$, measurements of V_s and ω/α should be interpreted with caution. The statistical uncertainty in V_s introduced by the streamer breakdown probability must be assessed. Space-charge acceleration of avalanche growth may affect measurements of ω/α.

ACKNOWLEDGMENTS

The voltage pedestal generator was designed and built by Dr. K. Bardin and Mr. K. Hing. We thank Dr. E. Hansen for assistance in the mathematical development. This research was supported by independent research and development funds of Lockheed Missiles and Space Company, Inc. (Palo Alto, CA).

APPENDIX

The approximation for the Bessel function[45]

$$I_1(z) \sim e^z/(2\pi z)^{1/2} \tag{A1}$$

is accurate to within 10% for $z > 2$. Substitution of this approximation yields the integral

$$\int_{n_c}^{\infty} V(n)dn = \tfrac{1}{2}\mu^{-3/4}(\bar{n}/\pi)^{1/2} \times \int_{n_c}^{\infty} n^{-3/2}\exp[-(1-\mu^{1/2})^2 n/\bar{n}]dn \ . \tag{A2}$$

The variable transformation $y = n^{1/2}$ gives the integral

$$\int_{n_c}^{\infty} V(n)dn = \mu^{-3/4}(\bar{n}/\pi)^{1/2} \int_{n_c^{1/2}}^{\infty} \exp[-(1-\mu^{1/2})^2 y^2/\bar{n}]y^{-2}dy \ , \tag{A3}$$

with solution[46]

$$\int_{n_c}^{\infty} V(n)dn = \mu^{-3/4}(\bar{n}/n_c)^{1/2}\{(e^{-x}/\pi^{1/2}) - x^{1/2}[1-\Phi(x^{1/2})]\} \ , \tag{A4}$$

where

$$x = (n_c/\bar{n})(1-\mu^{1/2})^2 \ , \tag{A5}$$

and the probability function

$$\Phi(z) = (2/\pi^{1/2}) \int_0^z e^{-t^2} dt \ . \tag{A6}$$

An analytical approximation for Φ is given by[45]

$$\Phi(x^{1/2}) = 1 - (a_1 t + a_2 t^2 + a_3 t^3)e^{-x} \ , \tag{A7}$$

where

$$t=1/(1+px^{1/2}) ,$$

$$p=0.470\,47 ,$$

$$a_1=0.348\,024\,2 ,$$

$$a_2=-0.095\,879\,8 ,$$

$$a_3=0.747\,855\,6 .$$

Inserting this approximation gives

$$\int_{n_c}^{\infty} V(n)dn=\mu^{-3/4}(\bar{n}/n_c)^{1/2}e^{-x} \times[\pi^{-1/2}-x^{1/2}(a_1t+a_2t^2+a_3t^3)] . \quad \text{(A8)}$$

[1]T. R. Burkes, M. O. Hagler, M. Kristiansen, J. P. Craig, W. M. Portnoy, and E. E. Kunhardt, *A Critical Analysis and Assessment of High-Power Switches,* Naval Surface Weapons Center Report No. NP30/78, Sept., 1978, available from Defense Technical Information Center, Alexandria, VA.

[2]C. M. Cooke in *Surges in High-Voltage Networks,* edited by K. Ragaller (Plenum, New York, 1980).

[3]C. Grey Morgan, in *Electrical Breakdown of Gases,* edited by J. M. Meek and J. D. Craggs (Wiley, New York, 1978), p. 655.

[4]J. S. Townsend, *The Theory of Ionization of Gases by Collision* (Constable, London, 1910).

[5]J. Dutton, Ref. 3, p. 216ff.

[6]E. E. Kunhardt, IEEE Trans. Plasma Sci. **PS-8**, 130 (1980).

[7]F. Llewellyn-Jones, in *Electrical Breakdown and Discharge in Gases,* edited by E. E. Kunhardt and L. H. Luessen (Plenum, New York, 1983).

[8]L. B. Loeb and J. M. Meek, *The Mechanism of the Electric Spark* (Stanford University, Stanford, 1941), p. 27ff.

[9]H. Raether, *Electron Avalanches and Breakdown in Gases* (Butterworth, London, 1964), Chap. 5.

[10]F. Llewellyn-Jones, *Ionization and Breakdown in Gases* (Wiley, New York, 1957), p. 78ff.

[11]F. Llewellyn-Jones, *Ionization, Avalanches, and Breakdown* (Methuen, London, 1967), p. 70ff.

[12]E. D. Lozanskii, Usp. Fiz. Nauk **117**, 493 (1975) [Sov. Phys.—Usp. **18**, 893 (1975)].

[13]E. E. Kunhardt and W. W. Byszewski, Phys. Rev. A **21**, 2069 (1980).

[14]R. A. Wijsman, Phys. Rev. **75**, 833 (1949).

[15]W. Legler, Z. Phys. **140**, 221 (1955).

[16]K. Richter, Z. Phys. **158**, 312 (1960).

[17]D. T. A. Blair, B. H. Crichton, and I. C. Somerville, in *Proceedings of the International Symposium on Gaseous Dielectrics,* edited by L. G. Christophorou (Oak Ridge National Laboratory, Oak Ridge, Tenn., 1978), p. 360.

[18]M. Laue, Ann. Phys. (Leipzig) **76**, 261 (1925).

[19]G. R. Govinda Raju and R. Hackam, J. Appl. Phys. **52**, 3912 (1981).

[20]M. Shimozuma, Y. Sakai, H. Tagashira, and S. Sakamoto, J. Phys. D **10**, 1671 (1977).

[21]J. Dutton, J. Phys. Chem. Ref. Data **4**, 577 (1975).

[22]L. E. Kline, D. K. Davies, C. L. Chen, and P. J. Chantry, J. Appl. Phys. **50**, 6789 (1979).

[23]C. Raja Rao and G. R. Govinda Raju, Int. J. Electron. **35**, 49 (1973).

[24]W. Legler, Z. Naturforsch. Teil A **16a**, 253 (1961).

[25]H. Tagashira, Proc. Phys. Soc. London **88**, 505 (1966).

[26]Y. Kondo, S. Kajita, and Y. Miyoshi, Denki Gakkai Ronbunshi **94A**, 530 (1974) [Elect. Eng. in Jpn. **94**, 27 (1974)].

[27]D. T. A. Blair and O. Farish, Br. J. Appl. Phys. **18**, 597 (1967).

[28]J. D. Swift and G. Collins, J. Phys. D **2**, 1047 (1969).

[29]P. Pech, Rev. Roum. Phys. **13**, 201 (1968).

[30]R. L. Farquhar, B. Ray, and J. D. Swift, J. Phys. D **13**, 2067 (1980).

[31]R. W. Crowe, J. Appl. Phys. **37**, 1515 (1966).

[32]G. R. Govinda Raju and M. S. Dincer, J. Appl. Phys. **53**, 8562 (1982).

[33]H. A Boyd and G. C. Crichton, Proc. Inst. Electr. Eng. **118**, 1872 (1971).

[34]W. Legler, Z. Naturforsch. Teil A **19a**, 481 (1964).

[35]I. S. Gradshteyn and I. M. Ryzhik, *Table of Integrals, Series, and Products* (Academic, New York, 1980), p. 712.

[36]K. R. Allen and K. Phillips, Proc. R. Soc. London, Ser. A **278**, 188 (1964).

[37]J. Pfaue, Z. Angew. Phys. **16**, 15 (1963).

[38]M. S. Bhalla and J. D. Craggs, Proc. Phys. Soc. London **80**, 151 (1962).

[39]Reference 5, p. 231.

[40]I. D. Chalmers, H. Duffy, and D. J. Tedford, Proc. R. Soc. London, Ser. A **329**, 171 (1972).

[41]J. L. Moruzzi, Br. J. Appl. Phys. **14**, 938 (1963).

[42]V. N. Maller and M. S. Naidu, IEEE Trans. Plasma Sci. **PS-3**, 49 (1975).

[43]R. N. Varney, H. J. White, L. B. Loeb, and D. Q. Posin, Phys. Rev. **48**, 818 (1935).

[44]A. J. Davies and C. J. Evans, Br. J. Appl. Phys. **16**, 57 (1965).

[45]*Handbook of Mathematical Functions,* U.S. Natl. Bur. Stand. (Applied Math. Ser. No. 55), edited by M. Abramowitz and I. A. Stegun (U.S. GPO, Washington, D.C., 1964).

[46]Reference 35, p. 337.